Modeling of Influence of Climate Change Character on the Territory of the Cryolithozone on the Value of Risks for the Road Network

Yu.V. Trofimenko (✉), A.N. Yakubovich, I.A. Yakubovich, E.V. Shashina
Moscow Automobile and Road Construction State Technical University (MADI),
Moscow, Russia
ywtrofimenko@mail.ru

Abstract—The level of climate risks is proposed to be estimated by the amount of thawing soil settlement in the formation of automobile roads, corresponding to the accepted scenario of the climate change. An updated algorithm is presented, according to which the average risk assessment for a 4-year period is divided into a risk assessment for individual years. Calculations performed for the climatic conditions of Yakutsk and Urengoy establish a significant dependence of the predicted risk on the warming pattern. The level of risk predicted when the average annual air temperature increases by 2 degrees is estimated as average (up to 526 points on a 1000-point scale). The most appropriate method of reducing this risk is to perform timely repairs to bring the road to the standard technical and operational condition without the use of special technologies for regulating the temperature regime of soil.

Keywords—Climate change, Road Network, Cryolithozone, Modeling, Soil Thawing, Climate Risks.

1 Introduction

1.1 Review of literature

In modern conditions, global climate change is a factor that has an apparent effect on the functional suitability of engineering linear objects operated in constant contact with the environment [1]. Regardless of how significant the contribution of man-made activities to the observed climate changes is (the diversity of opinions on this issue is very significant), the fact of such changes, in particular, the continued increase in air temperature in the atmospheric boundary layer, is not in doubt and requires measures to adapt objects to these changes [2]. Territories with permafrost or cryolitic soils are characterized by increased vulnerability to climate change (to the increase in average annual air temperatures) [3]. In these areas, the observed climate changes lead to the degradation of permafrost soils in the formation of linear structures, including the road network. The efficiency of subgrade soils reduction (as a result of intensive thawing of

the upper layer of permafrost) leads to the appearance of additional settlements of the thawing soil and deformation of road structures, which causes deterioration of their technical and operational properties up to destruction. In particular, numerous chaotically located road surface subsidence's naturally lead to the maximum possible traffic flow speed decrease and the road capacity reduction [4]. Possible empirical methods for evaluating the road surface condition parameters, in particular, its width, are described in [5]. The use of a multi-purpose radio-controlled car for this purpose is shown in [6].

Among the studies devoted to the influence of natural and climatic conditions on the technical and operational state of the road network, the following can be distinguished. In [7] it is shown that the express defect of the road slope (as a result of its erosion by the water flow of the increased intensity) leads to the accelerated pavement and road cross section damage; the road cross section resistance level to such external influence depends on the soil type and the slope angle. A new method for estimating seismic risk for transport networks with bridge structures using probabilistic seismic hazard analysis (seismic risk assessment based on the theorem of total probability) is given in [8]. The survival analysis of light cellular concrete used as part of the subgrade is performed in [9]. The method for survival assessing includes building a multi-level model for evaluating factors that affect the concrete functional performance (analytical hierarchy), building a membership function for each factor, and obtaining the final complex membership function for a parameter that quantitatively describes the survival (fuzzy integral assessment). In [10] a list of climatic and weather factors is formed, that have the most significant impact on the technical and operational condition of the road; and the structure of information-measuring system is proposed that can fix parameters values reflecting these factors in real time, and can forecast the technical and operational road condition on the basis of constantly updated data.

Quantitative forecasting of the subgrade settlement, taking into account the probabilistic nature of the factors affecting it, is performed in [11]. To overcome the weaknesses and limitations of purely probabilistic and purely deterministic models, a combined forecasting model is proposed and numerically implemented, based on an improved analysis of set pairs, and taking into account both stochastic and deterministic impacts on the subgrade soil. As a result, it is possible to quantify the amount of forecasted settlement at different levels of the probability of not exceeding this value. In [12], the development process of loess soil settlement is described quantitatively: its increase over time, starting from the moment of the first subgrade load application.

It should be noted that there are many methods used to forecast the soil settlement amount at the base of engineering constructions, and to provide a sufficiently high results accuracy. Subgrade settlement forecasting based on the regression of the reference vector of least squares and the quantum evolutionary algorithm is performed in [13]. A simplified method for settlement forecasting of pivot rings on reinforced cohesionless soils is given in [14].

In [15], the principles allowing to quantify the risks of road infrastructure objects (including road surface) malfunction in the territories of permafrost soils distribution, depending on the climate warming magnitude, are substantiated. The main parameter that determines the climate risk is thawing soil settlement value (additional settlement

as compared to that occurs in the climate before the warming beginning). Climate changes are described by a spasmodic increase in the average annual air temperature; as these changes have the probabilistic nature, warming is considered a normally distributed random variable with an average value of +2 °C and is described by a sample of several realizations. For each random variable realizations the expected additional soil settlement at the subgrade is determined and the climate risk is assessed; the final risk value is the settlement weighted average for all the considered realizations.

The forecast values of climate risk obtained in [15] are averaged over a sufficiently long period during which an increase in air temperature is simulated, and the realization order in the sample is not taken into account. Accordingly, the purpose of this work is to analyze in more detail the risks distribution within this period, and to obtain climate risk estimates for the most unfavorable dynamics of temperature changes, described using a sequence of random variable realizations that characterize the increase in the average annual air temperature for individual years of the simulated period.

1.2 Climate risk prediction technique

The main climatic parameters that affect the road network functionality decrease as a result of forecasted climate changes are the air temperature t, C, and the wind speed in the atmospheric boundary layer v, m/s. The quantitative values of these parameters are modeled at a pitch of $\Delta\tau$ for one full average year, the duration of which is assumed to be 365 days. Then, with the same pitch $\Delta\tau$, the heat exchange is modeled between atmospheric air and soil (the first type), and between individual fragments of the soil mass formed by the road cross section and the formation soil (the second type). Heat transfer of the first type is described by the empirical dependence of Matsumura:

$$Q_1 = 18v^{0,578}(t_a - t_g)S_g\Delta\tau, \tag{1}$$

where Q_l – the heat energy (J), v – the mean wind speed for the period $\Delta\tau$ (m/s); t_a and t_g – the average temperature of atmospheric air and ground surface, respectively (°C); S_g – square of design element of soil mass in contact with atmospheric air (m²).

The values of $Q_l > 0$ correspond to the heat flow into the soil, where the second type heat exchange models temperature dynamics in the road cross section and its formation. Then the modeled soil mass is divided into individual elements and the heat exchange of the second type between them is described by the formula:

$$Q_2 = \frac{\lambda_A + \lambda_B}{2\delta_x}(t_A - t_B)\delta_y\delta_z\Delta\tau, \tag{2}$$

where λ_A and λ_B – the temperature-dependent coefficients of soil thermal conduction for the contiguous design elements A and B (W/(m·°C)); δ_x, δ_y, δ_z – the designed soil elements dimensions along the x, y, and z axes (m); t_A and t_B – the average temperature of the design elements A and B, respectively (°C).

Based on the dependencies (1) and (2), the soil mass temperature dynamics during the average year is determined as a sequence of the individual design elements temperatures separated by time intervals $\Delta\tau$. Next, the soil state is detected at the maximum

(during the one year) thawing depth h_{max} (corresponding to the depth of penetration of the temperature isoline $t = t_{bf}$ into the soil, where the soil freezing temperature t_{bf} depends on soil type and humidity). Thus, the maximum thawing depth of the formation soil can be represented as:

$$h_{max} = M(\boldsymbol{T}, \boldsymbol{V}, \boldsymbol{G}), \tag{3}$$

where M – a generalized transformation operator (including, among others, a computational procedure for modeling the temperature dynamics of the formation soil); $\boldsymbol{T}$ – an array of atmospheric air temperature values throughout the year; $\boldsymbol{V}$ – an array of wind speed values; $\boldsymbol{G}$ – a set of geometric, physicomechanical, and thermophysical soil parameters.

The magnitude of the section or road network functionality loss risk expected when climate changes occur is considered to depend on the amount of excess soil thawing in the road formation, and on the additional settlement Δm caused by this thawing in the soil mass. To quantify Δm, two climate states are considered: the basic one, characterized by averaged values of $\boldsymbol{T}$ and $\boldsymbol{V}$ for the period 1960-1990, and the modified one, in which all values of atmospheric air temperatures are assumed to be increased by the same value of n (°C), resulting in an array of temperatures $\boldsymbol{T}^{(n)}$.

The base climate corresponds to the design and construction period of most of the currently operated highways in the cryolithozone of Russia; the changed climate reflects scenario assumptions about the road network operating conditions for the period up to 2030. The value of excess thawing during climate warming at n °C is defined as:

$$\Delta h^{(n)} = M(\boldsymbol{T}^{(n)}, \boldsymbol{V}, \boldsymbol{G}) - M(\boldsymbol{T}, \boldsymbol{V}, \boldsymbol{G}). \tag{4}$$

After that, taking into account the physicomechanical parameters of the soil, an additional settlement $\Delta m^{(n)}$ in the thawed soil layer with a thickness of $\Delta h^{(n)}$ is calculated.

The period during which additional thawing soil settlement is simulated and associated climate risks are determined consists of 4 consecutive years. The parameter n is considered a random normally distributed value, with an average value of $n_{med} = +2$ °C and a standard deviation of $\sigma = 0.85$ in order to take into account the variability of climate conditions for individual years. The climate warming is thus described by a sequence of values $\{n_1...n_4\}$, reflecting the atmospheric air temperature increase (compared to the base climate) for individual years of the modeled period.

The selection $\{n_1...n_4\}$ corresponding to the accepted values of n_{med} and σ is determined in sequence (see Fig. 1):

1. The range of possible values of n is divided into 4 sections with equal probability of getting the random variable realization within each of the sections; adjacent boundaries are determined from the conditions $F(n) = 0.25$, $F(n) = 0.5$ and $F(n) = 0.75$, where $F(n)$ is a function of the normal distribution;
2. Within each i-th section, the median value of n_i is determined, which is considered one of the implementations of the random variable n.
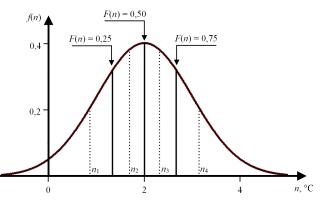
Fig. 1. The air warming value n_1–n_4 in individual years of the 4-year period under review

The resulting sample of 4 realizations of n, arranged in ascending order, has the form $\{n_1=0.86;\ n_2=1.686;\ n_3=2,316;\ n_4=3,142\}$ (values in C); the average value and the standard deviation of the sample coincide with n_{med} and σ. At the same time, there may be other implementations sequences in the sample that preserve the specified values of n_{med} and σ; there are 24 different sequences in total. Each sequence of n_i values reflects a particular variant of the atmospheric temperature dynamics over a 4-year period and, accordingly, one of the possible variations in climate risks during this period. To identify the most dangerous variant with the highest risks, all 24 n_i sequences are considered, and for each of them, risks are quantified by three indicators.

The first indicator $R_{1,i}$ reflects the risks expected in the i-th year of the period, and determined directly from the results of modeling additional formation soil settlement Δm_i, expressed in cm:

$$R_{1,i} = 100\Delta m_i. \tag{5}$$

The second indicator R_2 reflects the weight-average risk across all years of the period under review; considering the same probability for each of the implementations of n_i and hence the same probability for all values of Δm_i, the value of average risk is:

$$R_2 = 25 \sum_{i=1}^{4} \Delta m_i. \tag{6}$$

The third risk indicator $R_{3,i}$ is determined by the value Δm_i gradient: the specific settlement is calculated (corresponding to an increase in air temperature by +1 °C), which increases by the value of the average warming n_{med}:

$$R_{3,i} = 200 \frac{\Delta m_i}{n_i}. \tag{7}$$

The R_2 indicator reflects the most conservative estimation of the climate risk (lower estimate). The maximum value of $R_{3,i}$ for all years of the period, on the contrary, can be considered as the most pessimistic risk estimation (upper assessment). The indicator $R_{1,i}$, obviously, in most cases will give a risk forecast value, intermediate between the second and third indicators. The final conclusion about the expected climate risks value is formulated taking into account the values of all three indicators.

2 Results and Discussion

2.1 Numerical simulation results

Quantitative risk estimations performed for Yakutsk climatic conditions are shown in the Table 1, the values highlighted in the table correspond to the highest forecasted risk estimates for each of the three indicators R_1, R_2, and R_3. The road body (soil formation) height was assumed to be 2 m, the width at the top was 10 m, the formation soil was clay, with high humidity.

The forecast risks values for the road network (sections) in the Urengoy climate are shown in the Table 2, the geometric dimensions and physicomechanical parameters of the soil mass were assumed to be the same as for Yakutsk.

When performing all calculations, the modelling interval $\Delta\tau$ was assumed to be 1800 s; the geometric dimensions of the soil mass designed element were $\delta_x = \delta_y = \delta_z = 0.1$ m. Reducing the values of these modelling parameters did not lead to a significant change in the numerical results thus, the accuracy of the values in the tables 1 and 2 can be considered guaranteed.

Table 1. Forecast risks of the road network functionality decrease when the climate warms by 2 °C in the climatic conditions of Yakutsk

The temperature change dynamics by year	Annual risks $R_{1,i}$				Average risk for the entire period R_2	Risks defined by the gradient $R_{3,i}$			
n_1-n_2-n_3-n_4	49	239	346	458	274	113	283	298	294
n_1-n_2-n_4-n_3	49	239	373	393	263	113	283	238	339
n_1-n_3-n_2-n_4	49	325	301	458	283	113	281	357	292
n_1-n_3-n_4-n_2	49	325	381	327	272	113	281	247	388
n_1-n_4-n_2-n_3	49	442	312	357	283	113	264	371	308
n_1-n_4-n_3-n_2	49	415	366	321	288	113	264	316	380
n_2-n_1-n_3-n_4	208	182	285	**461**	284	246	423	246	293
n_2-n_1-n_4-n_3	208	182	439	390	305	246	423	279	337
n_2-n_3-n_1-n_4	208	335	213	452	302	246	289	496	288
n_2-n_3-n_4-n_1	208	335	456	227	306	246	289	290	521
n_2-n_4-n_1-n_3	208	361	159	354	271	246	230	369	306
n_2-n_4-n_3-n_1	208	361	357	163	272	246	230	308	378
n_3-n_1-n_2-n_4	241	192	289	396	280	208	446	343	252
n_3-n_1-n_4-n_2	241	192	442	250	281	208	446	281	297
n_3-n_2-n_1-n_4	241	241	210	451	286	208	286	489	287
n_3-n_2-n_4-n_1	241	241	452	226	290	208	286	287	**526**
n_3-n_4-n_1-n_2	241	439	163	307	288	208	280	379	364
n_3-n_4-n_2-n_1	241	439	244	217	286	208	280	290	505
n_4-n_1-n_2-n_3	354	203	294	365	304	226	473	349	316
n_4-n_1-n_3-n_2	354	203	294	317	292	226	473	254	376
n_4-n_2-n_1-n_3	354	298	144	353	287	226	354	335	305
n_4-n_2-n_3-n_1	354	298	352	158	291	226	354	304	367
n_4-n_3-n_1-n_2	354	351	219	305	307	226	303	510	362
n_4-n_3-n_2-n_1	354	351	314	216	**309**	226	303	372	503

2.2 Discussion

For all the considered variants of atmospheric temperature dynamics, high risk variability is forecasted for individual years of the 4-year period (indicators R_1 and R_3). According to the indicator R_1, this variability is slightly higher in Yakutsk conditions (the maximum change in risk over 4 years is 409 units). In Urengoy conditions, the R_1 risk value is also high (393 units). Risk estimates based on the gradient of settlement values R_3 have slightly less variability within the simulated period (the largest change over 4 years of the R_3 indicator is 318 units for Yakutsk and 254 units for Urengoy).

Table 2. Forecast risks of the road sections functionality decrease when the climate warms by 2 C in the climatic conditions of Urengoy

The temperature change dynamics by year	Annual risks $R_{1,i}$				Average risk for the entire period R_2	Risks defined by the gradient $R_{3,i}$			
n_1-n_2-n_3-n_4	119	195	312	**512**	284	276	231	269	326
n_1-n_2-n_4-n_3	119	195	491	409	303	276	231	312	353
n_1-n_3-n_2-n_4	119	343	293	430	296	276	284	347	273
n_1-n_3-n_4-n_2	119	343	429	308	300	276	284	273	365
n_1-n_4-n_2-n_3	119	424	300	397	310	276	270	356	343
n_1-n_4-n_3-n_2	119	424	399	319	315	276	270	344	378
n_2-n_1-n_3-n_4	227	166	374	436	300	269	385	323	277
n_2-n_1-n_4-n_3	227	166	484	408	321	269	385	308	353
n_2-n_3-n_1-n_4	227	360	183	429	300	269	311	426	273
n_2-n_3-n_4-n_1	227	360	505	225	329	269	311	322	**522**
n_2-n_4-n_1-n_3	227	426	189	391	308	269	271	440	338
n_2-n_4-n_3-n_1	227	426	403	212	317	269	271	348	492
n_3-n_1-n_2-n_4	304	173	286	505	317	263	403	339	321
n_3-n_1-n_4-n_2	304	173	489	329	324	263	403	311	391
n_3-n_2-n_1-n_4	304	286	181	429	300	263	339	421	273
n_3-n_2-n_4-n_1	304	286	501	223	328	263	339	319	517
n_3-n_4-n_1-n_2	304	480	204	299	322	263	306	475	354
n_3-n_4-n_2-n_1	304	480	306	190	320	263	306	363	441
n_4-n_1-n_2-n_3	429	183	290	395	323	269	425	344	341
n_4-n_1-n_3-n_2	429	183	385	306	324	269	425	332	363
n_4-n_2-n_1-n_3	429	296	129	313	290	269	352	300	270
n_4-n_2-n_3-n_1	429	296	395	209	**331**	269	352	341	486
n_4-n_3-n_1-n_2	429	390	189	242	311	269	337	439	287
n_4-n_3-n_2-n_1	429	390	302	201	327	269	337	359	466

The spread of risk values obtained taking into account possible differences in the dynamics of the temperature regime of atmospheric air in the territory of Yakutsk is: for the indicator R_1 – 30% ($R_{1,min}$=354, $R_{1,max}$=461), for the indicator R_2 – 17% ($R_{2,min}$=263, $R_{2,max}$=309), for the indicator R_3 – 77% ($R_{3,min}$=298, $R_{3,max}$=526). In Urengoy climatic conditions, the possible values spread is: for R_1 – 21% ($R_{1,min}$=424, $R_{1,max}$=512), for R_2 – 17% ($R_{2,min}$=284, $R_{2,max}$=331), for R_3 – 60% ($R_{3,min}$=326, $R_{3,max}$=522).

The high variability of risk estimates corresponding to different variants of possible atmospheric temperature dynamics indicates an underestimated level of climate risk

forecasted on the basis of averaged temperature parameters over the entire period. Only an analysis of all possible variations of temperature changes in the territory can reliably identify the maximum possible risk. It is also necessary to note the impact of the particular territory climatic features on the risk values, which is most noticeable in relation to R_1.

The maximum forecasted climate risk level obtained from numerical simulation is R_3=526 units and corresponds to the climate conditions of Yakutsk; in relation to the climatic features of Urengoy, the upper limit of the expected risk R_3 is at the level of 522 units. The qualitative interpretation of the risk values is described in [13]; according to it, the maximum risk, which means the complete functionality loss of the road section, corresponds to the value R=1000. The range of values $301 \leq R < 600$, to which the R_3 values belong for both examples considered, corresponds to the upper sublevel of the average risk. The lower risk estimate, based on weighted average values over a 4-year period, is R_2=331 for Urengoy and R_2=309 for Yakutsk; these values also allow to classify the risk as the average level one (lower sublevel).

3 Conclusion

The atmospheric air temperature dynamics influence on the risks level for roads sections (network) in the cryolithozone is significant and causes a change in the forecasted risk value from 17% to 77%. Identification of the most unfavorable temperature dynamics, at which the maximum road malfunction risk is forecasted, is an essential condition for obtaining reliable quantitative estimates of climate risks.

The risk level forecasted for road sections (network) in the area of Yakutsk and Urengoy, with the increase in the average annual air temperature as a result of climate warming up to +2 °C and the most dangerous nature of climate change, is estimated as average. This risk level involves constant monitoring of the road surface current state and timely repair works to eliminate defects that occur due to excessive soil formation thawing and settlement. The use of technologies for adaptation of road facilities that regulate the soil temperature regime (thermal insulation coatings, seasonal cooling devices) and prevent the occurrence of excess soil settlement is not mandatory for average risks. However, the final decision on the application of engineering measures to adapt specific roads sections in the regions under consideration should be made on the basis of detailed technical and economic calculations.

4 References

[1] Driga, A.M., Drigas, A.S. "Climate Change 101: How Everyday Activities Contribute to the Ever-Growing Issue", *International Journal of Recent Contributions from Engineering, Science & IT*, vol. 7(1), pp. 22-31, 2019. https://doi.org/10.3991/ijes.v7i1.10031

[2] Gruza, G.V. and et. "Features of the temperature regime at the surface of the globe in 2018", *Fundamental and Applied Climatology*,vol.pp. 97-127,2019.

[3] Anisimov, O., Kokorev, E., Zhiltcova, Y. "Arctic ecosystems and their services under changing climate: predictive-modeling assessment", *Geographical Review*, vol. 107(1), pp. 108-124, 2017 https://doi.org/10.1111/j.1931-0846.2016.12199.x

[4] Yakubovich, A.N., Trofimenko, Yu.V., Yakubovich, I.A., Shashina, E.V. "A forecast model for a road network's section traffic capacity assessment on a territory of the cryolithozone in conditions of the climate change", *Periodicals of Engineering and Natural Sciences*, vol. 7(1), pp. 275-280, 2019 https://doi.org/10.21533/pen.v7i1.380

[5] Nasution, S.M., Husni, E., Kuspriyanto, Yusuf, R., Mulyawan, R. "Road Information Collector Using Smartphone for Measuring Road Width Based on Object and Lane Detection", *International Journal of Interactive Mobile Technologies*, vol. 14(2), pp. 42-61, 2020 https://doi.org/10.3991/ijim.v14i02.11530

[6] Mahbub, M. "Design of a Multipurpose Radio Controlled Surveillance Vehicle to Monitor Risky Areas", *International Journal of Recent Contributions from Engineering, Science & IT*, vol. 7(2), pp. 7-29, 2019 https://doi.org/10.3991/ijes.v7i2.10380

[7] Ye, T., Xie, Q., Wang, Y., An, Y., Jin, J. "Analog modeling of sand slope stability with different precipitation conditions", *Journal of Modern Transportation*, vol. 26(3), pp. 200-208, 2018 https://doi.org/10.1007/s40534-018-0163-0

[8] Tak, H.-Y., Suh, W., Lee, Y.-J. "System-level seismic risk assessment of bridge transportation networks employing probabilistic seismic hazard analysis", *Mathematical Problems in Engineering*, vol. 2019, August, 2019. [Online serial]. Available: https://www.hindawi.com/journals/mpe/contents/year/2019/ [Accessed Apr.1, 2020] https://doi.org/10.1155/2019/6503616

[9] Liu, X., Ni, Ch., Zhang, L., Sheng, K., Hong, B. "Durability assessment of lightweight cellular concrete in subgrade by the method of analytic hierarchy process combined with fuzzy comprehensive evaluation", *Mathematical Problems in Engineering*, vol. 2019, August, 2019.[Online serial].Available:https://www.hindawi.com/journals/mpe/contents/year/2019/ [Accessed Apr. 1, 2020] https://doi.org/10.1155/2019/4915870

[10] Yakubovich, A.N., Yakubovich, I.A., Trofimenko, Yu.V., Shashina, E.V. "Intelligent management system of the automobile road's technical and operational condition in the cryolithozone", in Proc. Systems of Signals Generating and Processing in the Field of on Board Communications, SOSG 2019'03 2019 https://doi.org/10.1109/sosg.2019.8706742

[11] Li, Y., Leng, W., Nie, R., Mei, H., Zhou, S., Dong, J. "A combined prediction model for subgrade settlement based on improved set pair analysis", *Mathematical Problems in Engineering*, vol. 2019, August, 2019. [Online serial]. Available: https://www.hindawi.com/journals/mpe/contents/year/2019/ [Accessed Apr. 1, 2020] https://doi.org/10.1155/2019/1064246

[12] Ge, M., Li, N., Zhang, W., Zheng, J., Zhu, C. "Settlement behavior and inverse prediction of post-construction settlement of high filled loess embankment", *Chinese Journal of Rock Mechanics and Engineering*, vol. 36(3), pp. 745–753, 2017

[13] Gao, H., Song, Q.-C., Huang, J. "Subgrade settlement prediction based on least square support vector regession and real-coded quantum evolutionary algorithm", *International Journal of Grid and Distributed Computing*, vol. 9(7), pp. 83–90, 2016 https://doi.org/10.14257/ijgdc.2016.9.7.09

[14] Tafreshi, S.N.M., Shaghaghi, T., Mehrjardi, G.T., Dawson, A.R., Ghadrdan, M. "A simplified method for predicting the settlement of circular footings on multi-layered geocell-reinforced non-cohesive soils", *Geotextiles and Geomembranes*, vol. 43(4), pp. 332–344, 2015 https://doi.org/10.1016/j.geotexmem.2015.04.006

[15] Yakubovich, A., Trofimenko, Yu., Pospelov, P. "Principles of developing a procedure to assess consequences of natural and climatic changes for transport infrastructure facilities in

permafrost regions", *Transportation research procedia*, vol. 36, pp. 810-816, 2018. https://doi.org/10.1016/j.trpro.2018.12.076

5 Authors

Yury Vasilievich Trofimenko is the head of the Technosphere Safety Chair of Moscow Automobile and Road Construction State Technical University (MADI), Leningradsky avenue, 64, Moscow, Russia, 125319.E-mail: ywtrofimenko@mail.ru

Anatoly Nikolaevich Yakubovich is a full professor of the Operation and Servicing of Motor Vehicles Chair of Moscow Automobile and Road Construction State Technical University (MADI), Leningradsky Avenue, 64, Moscow, Russia, 125319.

Irina Anatolievna Yakubovich is a full professor of the Operation and Servicing of Motor Vehicles Chair of Moscow Automobile and Road Construction State Technical University (MADI), Leningradsky Avenue, 64, Moscow, Russia, 125319.

Elena Vladimirovna Shashina is an assistant professor of the Technosphere Safety Chair of Moscow Automobile and Road Construction State Technical University (MADI), Leningradsky Avenue, 64, Moscow, Russia, 125319.